

Dual parameters discrimination comparison between two types of optical fiber sensors during the operation of a Li-ion battery

Lucca C. Matuck*^a, João L. Pinto^a, Carlos A. F. Marques^a, Micael S. Nascimento^a

^aDepartment of Physics, University of Aveiro, Campus de Santiago 3810-193 Aveiro, Portugal

ABSTRACT

In this work, a comparison between the temperature and strain decoupling performed by a bare polarization-maintaining FBG (PM-FBG) sensor and by a hybrid sensing setup, involving the slow peak of the PM-FBG and the fringe shift of the fiber loop mirror (FLM) interferometer (FLM+FBG_{slow}), was studied and discussed. To promote such comparison, the sensors were submitted to temperature and strain variations at the surface of a cylindrical Li-ion battery (LiB), cycling between 3.0 V and 4.2 V. The data spread of the FLM+FBG_{slow} indicates a root mean square deviation of ± 0.1 °C and ± 7.8 $\mu\epsilon$, against ± 0.5 °C and ± 9.7 $\mu\epsilon$ in PM-FBG, for temperature and strain, respectively. The matrixial method through the sensitivities values of each sensor was used for data processing. Although both sensing configurations showed similar trend behavior of strain and temperature variations during all the experiment, the FLM+FBG_{slow} setup presented better accuracy when compared to the PM-FBGs, however, it could only perform measurements in all the LiB extension, while the PM-FBG could provide data regarding a specific spot of the LiB. The highest temperature and strain variations were achieved in the end of the discharge processes.

Keywords: Fiber loop mirror, polarization-maintaining fibers, temperature and strain, Li-ion batteries monitor.

1. INTRODUCTION

The control and management of Li-ion batteries (LiB) critical parameters have received considerable attention due to the challenge to improve the efficiency, usability, and safety of such devices in their massive usability for the green energy transition [1]. In the last years, several types of sensors have been attached to LiBs to perform measurements regarding, such as temperature, strain, static pressure, and refractive index changes [2–4]. One of the most used in such application, are the fiber Bragg grating (FBG) sensors, due to their well-known intrinsic capabilities and advantages [5]. However, FBG sensors present high cross-sensitivity phenomenon, indicating that such sensors are sensible to multiple parameters simultaneously, presenting the benefit to allow multiple parameters measurements with one sensor head, but the necessity to develop a good strategy to decouple the effects of such parameters in real applications can be a challenge.

In FBG sensors inscribed in high birefringent (Hi-Bi) fibers, commonly named polarization-maintaining FBG (PM-FBG), two propagation modes shall be observed (fast (y-axis) and slow (x-axis) modes), thus, two Bragg reflections peaks as well, one for each propagation mode are presented. Each Bragg reflection peak present different sensitivity values for the same parameter due to the different stress conditions on the x and y-axis in the PM fiber, the light traveling within the fiber is submitted to different refractive index, a phenomenon known as birefringence, inducing two propagations modes. Thus, in applications using PM-FBG sensors, a simple dual-parameter decoupling can be performed by using the matrixial method though the obtained sensitivities. PM-FBG sensors were already used to decouple strain and temperature variations in a battery shell surface [6]. Fiber loop mirror (FLM) sensors have been also reported in the literature to simultaneous discriminate parameters [7-8]. They consist in an interferometer where a Hi-Bi fiber is spliced between single mode fibers (SMF). When the Hi-Bi filament suffer variations from the environment, the interference spectrum response of the sensor shifts, allowing the characterization to such variations. In 2014 Wang et al. demonstrated a hybrid sensor composed by a FLM and a PM-FBG sensor to decouple temperature and strain variations [8]. Such hybrid sensor has never been applied in a real application to simultaneously discriminate such parameters in order to know if they really promote this sensing, and what measurand errors are associated with each different discrimination process.

In this work, it is intended to compare and evaluate both discrimination methodologies (PM-FBG vs FLM+PM-FBG_{slow}) in terms of measurand errors and accuracy, between the sensing of temperature and strain parameters by inscribing a FBG in PM fibers of a FLM, in a real scenario, i.e., during a cylindrical LiB operation in charge/discharge cycles.

2. EXPERIMENTAL SETUP

For the sensor development a commercial photosensitive Hi-Bi PANDA fiber (PS-PM980, Thorlabs Inc., Newton, MA, USA) with birefringence index of 2.8×10^{-4} was used. Aiming to improve the photosensitivity and record more reflective PM-FBG, a 6.5 cm PANDA optical fiber line was hydrogenated at 120 bar during one week. Then the filament was spliced in both edges of SMFs, performing the FLM. After that, the PM-FBG sensor was inscribed in the middle of the PANDA filament by a pulsed Q-switched Nd:YAG laser system (LOTIS TII LS-2137U Laser, Minsk, Belarus) lasing at the fourth harmonic (266 nm) and focusing the beam in the fiber with a plano-convex cylindrical lens (working length of 320 mm) during 15 min creating in this way a hybrid sensor (FLM+PM-FBG). The hybrid sensor is illustrated in Figure 1 a) and the spectrum response of the optical sensor can be observed in Figure 1 b).

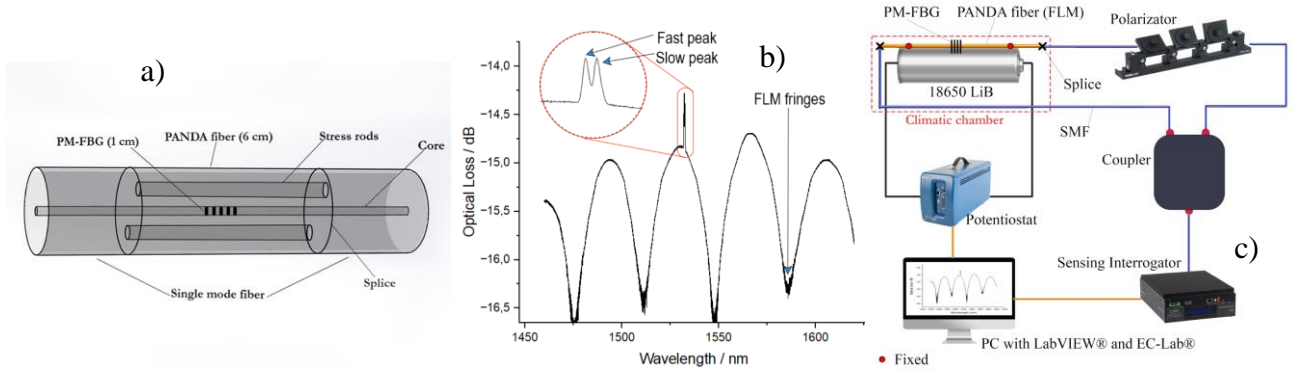


Figure 1. a) Illustration of the hybrid sensor. b) Spectrum response of a hybrid sensor composed by a FLM and PM-FBG sensors. The PM-FBG was reflective enough to stand out the FLM spectrum, allowing the usage in applications of simultaneous temperature and strain variations. c) Representative scheme of all components used in the experiment. A 65 mm PANDA optical fiber line was used, the distance between the fixed points was 60 mm, where the FLM interferometer is produced between the splices.

The battery used was a commercial rechargeable ICR18650 S3 2200 mAh LiB (18x65 mm) with nominal voltage of 3.6 V, operating in the horizontal direction. The spectrum response of the hybrid sensor was measured by an optical interrogator (Hyperion si155 Optical Sensing Instrument, Luna®, VA, USA) operating at 100 Hz and wavelength accuracy of 1.0 pm. A 50:50 optical coupler and a polarization controller were necessary to control and adjust the FLM response spectrum. The Biologic SP-50e potentiostat was used to perform the galvanostatic cycling steps. The charging and discharging steps were performed at 1.0 A (0.45 C rate) constant current until achieved 4.2 V and 3.0 V, respectively. The discharge steps were performed at 1.0 A constant current during all the process. The electrical data were recorded also by the potentiostat. A 15-minute resting time were given after each process, allowing the temperature stabilization of the battery. The Enlight® software managed the data logging of the optical interrogator, and the EC-Lab®, the electrical battery data. During all the tests, the battery instrumented with optical fiber sensors was kept in a constant 25.0 °C temperature environment, within the climatic chamber (model LC64, from WeissTechnik, Supplylab, Lisbon-Portugal). The setup is represented and illustrated in Figure 1 c). The hybrid sensor, was fixed in the external surface of the edges of the cylindrical battery ($L= 60$ mm), being the PM-FBG located in the center of the battery and the FLM measuring all the superficial temperature variations.

The matrixial method through the sensitivities values of each sensor was used for data processing, as shown in Equation 1. The \mathbf{K} matrix is composed by the sensitivity constants to temperature and strain parameters, where K_1 and K_2 represent the sensitivity of two different sensors for temperature (T) and strain (ϵ), and D is the determinant value. The variations of temperature (ΔT) and strain ($\Delta \epsilon$) may be decoupled by solving the matrixial equity, where $\Delta \lambda_1$ and $\Delta \lambda_2$ represent the wavelength shifts of each sensor. For that, it has been followed the PM-FBG peaks and the FLM fringes in the spectral response.

$$\begin{pmatrix} \Delta \lambda_1 \\ \Delta \lambda_2 \end{pmatrix} = \begin{pmatrix} K_{\epsilon 1} & K_{T 1} \\ K_{\epsilon 2} & K_{T 2} \end{pmatrix} \begin{pmatrix} \Delta \epsilon \\ \Delta T \end{pmatrix} = \mathbf{K} \begin{pmatrix} \Delta \epsilon \\ \Delta T \end{pmatrix}, \quad \begin{pmatrix} \Delta \epsilon \\ \Delta T \end{pmatrix} = \frac{1}{D} \begin{bmatrix} K_{T 2} & -K_{T 1} \\ -K_{\epsilon 2} & K_{\epsilon 1} \end{bmatrix} \begin{pmatrix} \Delta \lambda_1 \\ \Delta \lambda_2 \end{pmatrix} \quad (1)$$

3. RESULTS AND DISCUSSION

For the temperature and strain decoupling process, two methods were studied and compared, one involving the FLM and the slow mode Bragg reflection (FLM+FBG_{slow}) and the other, through the double peaks of the PM-FBG (FBG_{slow}+FBG_{fast}). The sensitivities and resolutions were determined when subjected to strain and temperature shifts with ranges of $\sim 1700 \mu\epsilon$ ($\sim 150 \mu\epsilon$ steps) and $25.0 \text{ }^\circ\text{C}$ ($5.0 \text{ }^\circ\text{C}$ steps), respectively. From the results shown in Figure 2a) and 2b), higher sensitivity values were obtained for the FLM, of $-1534.67 \pm 5.02 \text{ pm}/^\circ\text{C}$ and $12.09 \pm 0.05 \text{ pm}/\mu\epsilon$. The spread of the data in the matrices calculated though Equation 1, indicates root mean square (RMS) deviations of, $\pm 0.5 \text{ }^\circ\text{C}$ and $\pm 9.7 \mu\epsilon$ and $\pm 0.1 \text{ }^\circ\text{C}$ and $\pm 7.8 \mu\epsilon$ for temperature and strain measurements from the simultaneously discrimination of the PM-FBGs (Figure 2c)) and FLM+FBG_{slow} (Figure 2 d)) sensing configurations, respectively.

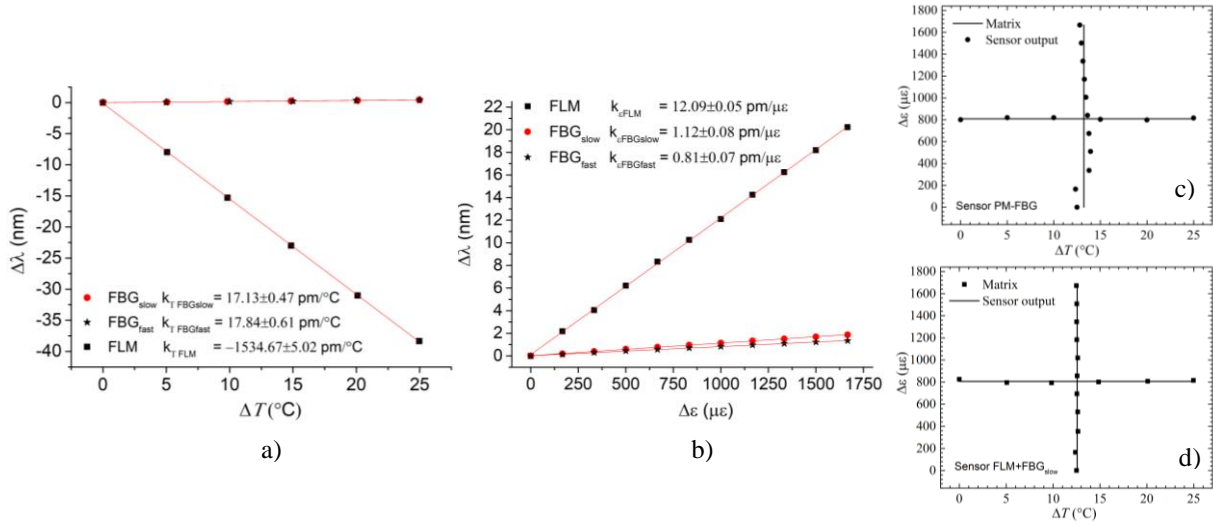


Figure 2. Sensors' characterization to temperature (a) and strain (b) variations. FLM presents higher sensitivity to both parameters. Cross-matrix for PM-FBG (c) and for FLM+FBG_{slow} (d) methods.

During the galvanostatic cycling tests (Figure 3, left), the temperature variations detected by the FLM+FBG_{slow} hybrid method was lower when compared to the PM-FBG method, due the fact of the FLM reach out the entire extension of the battery surface and the PM-FBG sensor only the middle area, where the temperature variation tends to be higher. However, the FLM+FBG_{slow} presents very low output signal fluctuations (higher accuracy) in comparison with the PM-FBG method. Regarding the strain discrimination (Figure 3, right), more accurate and refined data was also obtained by using the FLM+FBG_{slow} method.

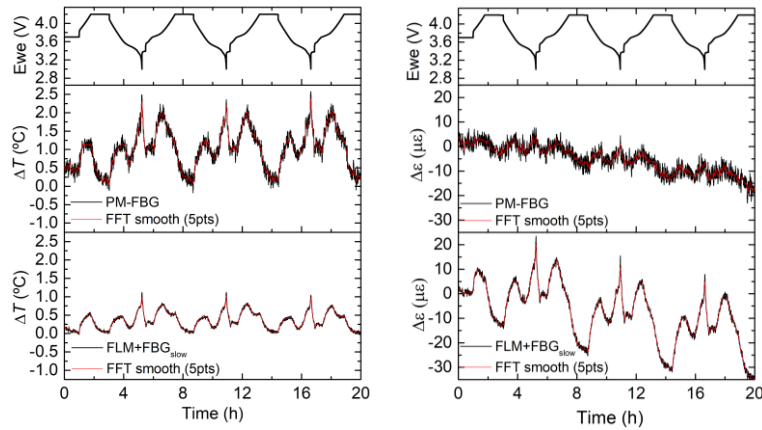


Figure 3. Temperature (left) and strain (right) variations of the battery during the galvanostatic cycling tests over time. The terminal voltage of the battery can be associated with the battery cell temperature and strain variation.

From the simultaneous discrimination, the maximum temperature and strain shifts were recorded in the end of the discharge process, when the terminal cell voltage was around the cut-off voltage, 3.0 V, due to the thermal expansion of the internal

LiB components. By using the PM-FBG, considerable low strain changes were detected in comparison with the FLM+FBG_{slow} method, however both signals show similar behaviors over all the galvanostatic cycles. In general, a LiB relaxation was detected over the 3 cycles and the strain data of the FLM+FBG_{slow} presented better and more reliable resolution while the PM-FBG method data indicates a trend behavior of the strain but it can't reliably quantify the strain variation. As the sensitivities determined for the FLM are higher than those determined for the PM-FBGs, the decoupling by using the hybrid sensor method (FLM+PM-FBG_{slow}) shall be consistent and with lower errors when compared to a bare PM-FBG method. However, the PM-FBG have an advantage to track the parameters in a specific point, while the FLM is based in all their length. The approach to use both Bragg reflections from the PM-FBG sensor represent an easy approach to perform temperature and strain decoupling, however, the close resolution to strain and temperature is a challenge to produce reliable quantitative data, mainly for strain variation.

4. CONCLUSIONS AND FUTURE WORK

A comparison between two methods based on PM-FBG vs FLM+PM-FBG_{slow} for simultaneous discrimination of temperature and strain changes was successfully performed in this study over a real scenario over operation of a LiB. Both techniques provided acceptable decoupling of both parameters, with the advantage to inscribe a PM-FBG in the Hi-Bi fiber of the FLM, to use only one optical fiber line. The LiB temperature and strain variations are in accordance with previous works reported in literature [9-10]. The results from FLM+FBG_{slow} show lower RMS deviations and a reliable setup measurement of strain and temperature variations during LiB operation. being an alternative approach to improve reliable quantitate data, mainly regarding their strain variations. As future work, FLM length can be adjusted in order to obtain a highest punctual temperature detection and integrated inside pouch cell LiB for internal strain tracking.

ACKNOWLEDGEMENTS

The authors gratefully acknowledge the European Project “Innovative physical/virtual sensor platform for battery cell” (INSTABAT) (European Union’s Horizon 2020 research and innovation programme under grant agreement No 955930), grant number BI/UI96/9971/2022, <https://www.instabat.eu/>. INSTABAT project is on umbrella of BATTERY2030+ roadmap. The authors also acknowledge the financial support within the scope of the project i3N, UIDB/50025/2020 & UIDP/50025/2020, financed by national funds through the FCT/MEC.

REFERENCES

- [1] J. Amici *et al.*, “A Roadmap for Transforming Research to Invent the Batteries of the Future Designed within the European Large Scale Research Initiative BATTERY 2030+,” *Adv Energy Mater*, vol. 12, no. 17, 2022, doi: 10.1002/aenm.202102785.
- [2] A. Nedjalkov *et al.*, “Refractive index measurement of lithium ion battery electrolyte with etched surface cladding waveguide bragg gratings and cell electrode state monitoring by optical strain sensors,” *Batteries*, vol. 5, no. 1, 2019, doi: 10.3390/batteries5010030.
- [3] W. Ren *et al.*, “Characterization of commercial 18,650 Li-ion batteries using strain gauges,” *J Mater Sci*, vol. 57, no. 28, pp. 13560–13569, 2022, doi: 10.1007/s10853-022-07490-4.
- [4] S. Huang *et al.*, “In Situ Measurement of Lithium-Ion Cell Internal Temperatures during Extreme Fast Charging,” *J Electrochem Soc*, vol. 166, no. 14, pp. A3254–A3259, 2019, doi: 10.1149/2.0441914jes.
- [5] G. Han, *et al.*, “A review on various optical fibre sensing methods for batteries,” *Renewable and Sustainable Energy Reviews*, vol. 150, p. 111514, Oct. 2021, doi: 10.1016/J.RSER.2021.111514.
- [6] L. Matuck, *et al.*, “Simultaneous Strain and Temperature Discrimination in 18650 Li-ion Batteries Using Polarization-Maintaining Fiber Bragg Gratings,” *Batteries*, vol. 8, no. 11, p. 233, 2022, doi: 10.3390/batteries8110233.
- [7] D. Leandro and M. Lopez-Amo, “All-PM Fiber Loop Mirror Interferometer Analysis and Simultaneous Measurement of Temperature and Mechanical Vibration,” *Journal of Lightwave Technology*, vol. 36, no. 4, pp. 1105–1111, 2018, doi: 10.1109/JLT.2017.2761121.
- [8] Q. Wang *et al.*, “Simultaneous measurement of strain and temperature with polarization maintaining fiber Bragg grating loop mirror,” *Instrum Sci Technol*, vol. 42, no. 3, pp. 298–307, 2014, doi: 10.1080/10739149.2013.865213.
- [9] M. Nascimento, *et al.*, “Thermal mapping of a lithium polymer batteries pack with FBGs network,” *Batteries*, vol. 4, no. 4, Dec. 2018, doi: 10.3390/batteries4040067.
- [10] J. Peng, *et al.* “Design and investigation of a sensitivity-enhanced fiber Bragg grating sensor for micro-strain measurement,” *Sens Actuators A Phys*, vol. 285, pp. 437–447, 2019, doi:10.1016/j.sna.2018.11.038.